

Coupling Bubble and Material Dynamics to Model Cavitation Peening and Pitting

Georges L. Chahine¹, Chao-Tsung Hsiao¹, Anil Kapahi¹, and Jin-Keun Choi¹

¹DYNAFLOW, INC.

10621-J Iron Bridge Rd, Jessup, MD, 20794, USA

ABSTRACT

The effects of cavitation bubbles dynamics on material peening and pitting are investigated numerically using a coupled incompressible/compressible fluid and material mechanics approach. The model is illustrated here on peening and pitting of Al 7075 following nonspherical cavitation bubble collapse near the material. Bubble reentrant jet impact and shock wave emissions from the jet impact and from the collapse of the remaining bubble ring can induce permanent micro-deformation (pitting) and residual stresses, which modify the roughness of the material and harden it through pre-stressing.

1. Introduction

Cavitation is known for its deleterious effects such as material damage and erosion. However, operating conditions can be selected to result in beneficial results such as material cleaning or strengthening through peening. When bubbles implode on material surfaces they develop high speed reentrant jets and emit shock waves, which result in high stress waves propagating into the material [1,2]. When the intensity of these waves exceeds the yield strength of the material, permanent deformation and residual stresses remain in the material. This can increase the yield strength of the material and harden it [3]. This loading mechanism - cavitation peening - can be done in a controlled manner to increase the life of the material against fatigue. This phase of accumulation of residual stress is also related to the incubation period of material erosion and pitting [1,2]. Therefore, depending upon the intensity of the cavitation and the duration of the exposure, the result can lead to desired residual stresses improving the fatigue life of material or to damaging erosion and mass loss. The reentrant jet and flow field formed during the bubble collapse can also be used for micro-particle cleaning [4].

2. Method

The numerical approach to model the coupled bubble/material dynamics is part of a general hybrid approach which we developed to simulate fluid structure interaction (FSI) problems involving shock waves and highly deforming bubbles [1,2]. The bubble growth phase and the reentrant jet development are handled with a highly accurate Boundary Element Method (BEM) [5]. Reentrant jet impact on the other side of the bubble or on the material and the following bubble ring collapse can result in shock wave formation and are handled using a compressible flow solver [6], which seamlessly continues the BEM solution using a link procedure [1,2]. This hybrid procedure is an efficient way of handling bubble dynamics near boundaries without compromising the physics of the problem. The dynamics of the material is modelled using the finite element model DYNA3D [7]. In the examples given below, Al 7075 is used to illustrate cavitation peening and pitting. This aluminum alloy is modeled using a bilinear elastic-plastic model with two slopes (moduli), one for the initial elastic regime and the second, a tangent modulus, for the plastic regime [1,2].

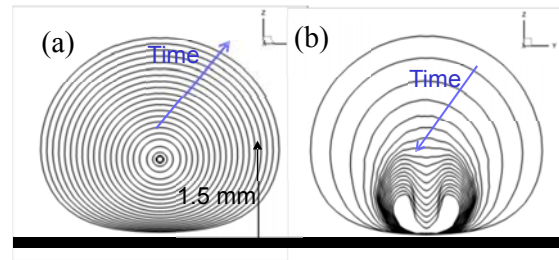


Fig. 1 Bubble shape during (a) growth and (b) collapse. 3DYNAPS-BEM results: $R_0=50 \mu\text{m}$, $X=1.5 \text{ mm}$.

3. Results and Discussion

To illustrate bubble / material dynamics, we consider a bubble of radius $R_0=50 \mu\text{m}$ in equilibrium at 100 KPa with the surrounding liquid, and subject it to a pressure drop to 1 KPa for 2.4 ms followed by a pressure rise to $P_d=10 \text{ MPa}$. As shown in Fig. 1 from the BEM solution, this results in the bubble expansion to an equivalent radius $R_{max}=2\text{mm}$ followed by a strong collapse with reentrant jet formation and pressure loading of the nearby Al 7075 plate located at a standoff of $X=1.5 \text{ mm}$.

The BEM solution at the moment of touchdown is then mapped to the compressible flow solver, which computes the dynamics of the multi-connected bubble and couples it with the material dynamics to provide the stresses in the material as shown in Fig. 2. A high pressure wave is emitted when the jet impacts the other side of the bubble (Fig. 2a) and then the wall (Fig. 2c). Another high pressure and shock waves are emitted with the remaining bubble ring collapses (Fig. 2d). These instantaneous high loads induce high stresses to substantial depths in the material illustrated in Fig. 2e-h.

The displacement of the central node of the plate along with the pressure recorded at that location is shown in Fig. 3. Note that there is a sharp rise in pressure due to reentrant jet impact. The resulting bubble ring collapses with even higher pressure at $1.5 \mu\text{s}$ as seen in the figure.

The contours of residual stress in the peened material are shown Fig. 4a. The figure also indicates the increase in roughness due to the formation of a microscopic pit under the bubble. Details of this dynamics can be found in [1,2]. The resulting roughness of the surface is negligible compared to solid body collision [3]. Finally, the temporal variation of residual stress developed in the material along the depth is shown in Fig. 4b.

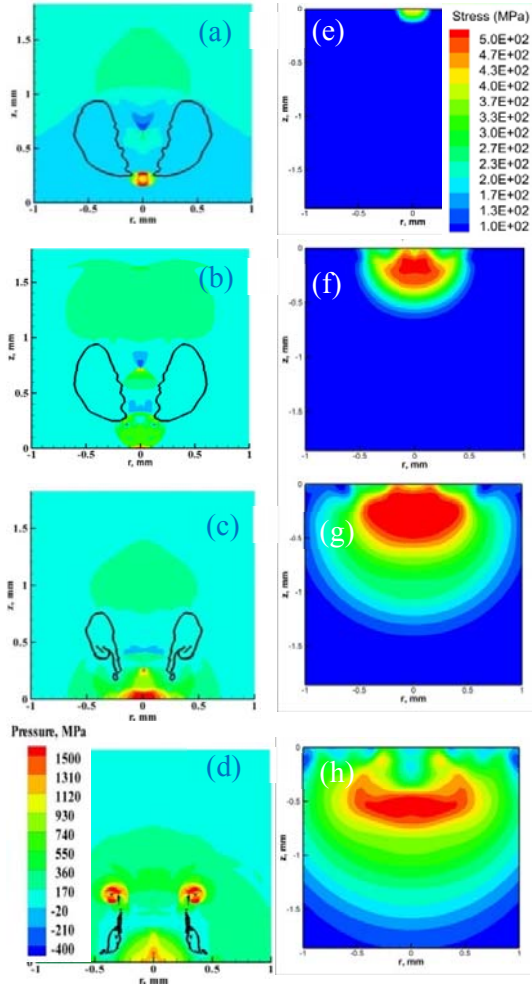


Fig. 2 Liquid pressures and material stress contours during bubble collapse after reentrant jet impact.

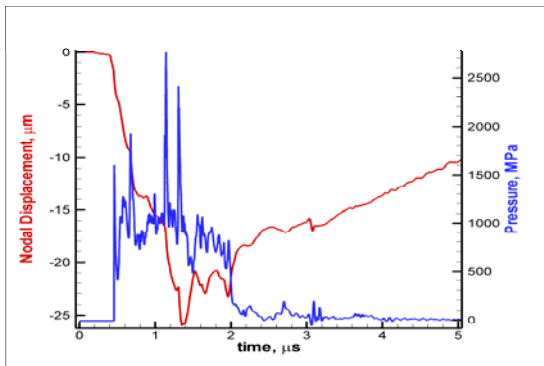


Fig. 3 Nodal displacement and pressure for $R_o = 50 \mu\text{m}$, $R_{\text{max}} = 2 \text{ mm}$, $P_d = 10 \text{ MPa}$ and $X=1.5 \text{ mm}$.

Note that the residual compressive stress saturates with time and can increase the yield strength of the material.

4. Concluding Remarks

Modeling coupled bubble and material dynamics and interactions provides a powerful method to investigate cavitation bubble characteristics needed to study

cavitation erosion or to design effective peening or cleaning techniques. This contribution illustrates what information can be obtained in such investigations.

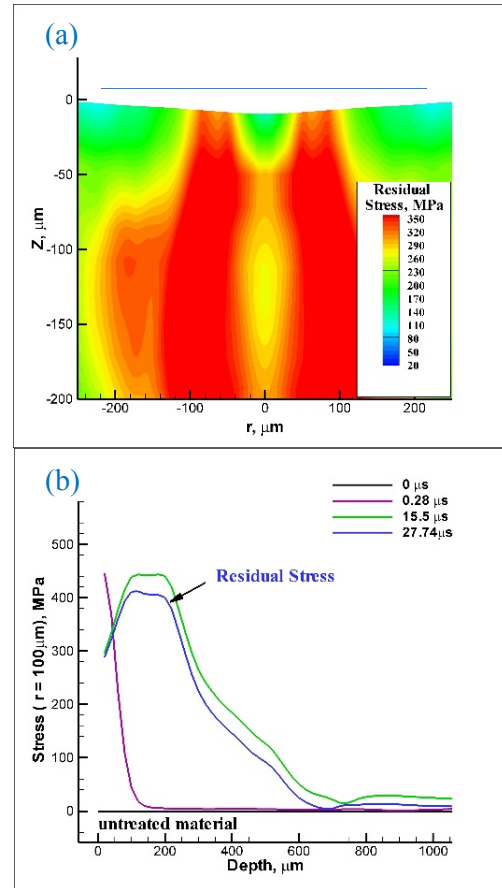


Fig. 4 (a) Residual equivalent stress in the material and pit shape. (b) Residual stress with depth at different times.

References

- [1] G. L. Chahine, in *Advanced Experimental and Numerical Techniques for Cavitation Erosion Prediction*, A. Kim, et al., Ed. Berlin, Chap. 6, Springer (2014) 123–173.
- [2] C.-T. Hsiao, A. Jayaprakash, A. Kapahi, J.-K. Choi, and G. L. Chahine, *J. Fluid Mech.* vol. 755, (2014) 142–175.
- [3] D. Odhiambo, *Int. J. Fatigue* vol. 25, no. 9–11, (2003) 1217–1222, Sep.
- [4] G. L. Chahine, A. Kapahi, J.-K. Choi, and C.-T. Hsiao, *Ultrason. Sonochem.* vol. 10.1016/j., (2015) May.
- [5] G. L. Chahine and K. Kalumuck, *Int. J. Comput. Appl. Technol.* vol. 11, no. 3–5, (1998) 177–198.
- [6] A. Kapahi, C.-T. Hsiao, and G. L. Chahine, *Comput. Fluids*, 10.1016/j.compfluid.2015.03.016. (2015)
- [7] R. G. Whirley and B. E. Engelmann, *Lawrence Livermore Natl. Lab.* no. UCRL-MA-107254, Rev.1 (1993).